T. QIU[1,2]
X.L. WU[1,✉]
Y.F. MEI[2]
P.K. CHU[2]
G.G. SIU[2]

Self-organized synthesis of silver dendritic nanostructures via an electroless metal deposition method

[1] National Laboratory of Solid State Microstructures and Department of Physics, Nanjing University, Nanjing 210093, P.R. China
[2] Department of Physics & Materials Science, City University of Hong Kong, Kowloon, Hong Kong, P.R. China

ABSTRACT Unique silver dendritic nanostructures, with stems, branches, and leaves, were synthesized with self-organization via a simple electroless metal deposition method in a conventional autoclave containing aqueous HF and $AgNO_3$ solution. Their growth mechanisms are discussed in detail on the basis of a self-assembled localized microscopic electrochemical cell model. A process of diffusion-limited aggregation is suggested for the formation of the silver dendritic nanostructures. This nanostructured material is of great potential to be building blocks for assembling mini-functional devices of the next generation.

PACS 61.46.+w; 68.70.+w; 81.65.Cf

In the past two decades, fractal structures of noble metals, including metal–polymer composites, have attracted much attention [1–4]. Fractals are generally observed in non-equilibrium growth processes; they can therefore provide a natural framework for the study of disordered systems. The diffusion-limited aggregation (DLA) model [5] and the cluster–cluster aggregation model [6] have been widely used to explain and analyze these fractal phenomena. Recently, a few methods have been devoted to the preparation of silver nanostructures with fractal morphologies [7–9], because the performance of silver in most of the applications ranging from electronics and catalytics to photonics [10] could significantly be enhanced by processing silver into nanostructures with well-controlled dimensions [11]. In general, fractal (randomly ramified) growth is expected when randomness dominates, whereas dendritic (symmetrically branched) growth is caused by the anisotropy [5, 6]. Accordingly, either fractal or dendritic nanostructures depend on exact growth conditions. Because controlled size and symmetrical shape of silver nanostructures are favorable for their properties and applications, some workers have investigated the crossover from fractal to dendritic silver patterns [12, 13]. However, synthesis of symmetrically branched or shapely dendrites is still a challenge.

In this paper, we report the synthesis of unique silver dendritic nanostructures, with stems, branches, and leaves, via a simple electroless metal deposition method in a conventional autoclave containing aqueous HF and $AgNO_3$ solution. Electroless metal deposition in ionic metal (silver) HF solution is based on a microelectrochemical redox reaction in which both anodic and cathodic processes occur simultaneously at the silicon surface [14]. This is a simple and inexpensive fabrication technique and has been widely used in microelectronics and the metal-coating industry [15–17].

The synthesis procedure includes pre-nucleation of silver nanoparticles inside the pores of an etched silicon wafer as seeds and on the apex of formed silicon nanowires, and subsequently self-organized growth of silver dendritic nanostructures. This nanostructured material is of great potential to be building blocks for assembling mini-functional devices of the next generation.

The sample-fabrication method is described as follows: a p-type, B-doped silicon (100) (1–5 Ω cm) wafer was first cleaned by acetone to degrease the Si surface, followed by etching in diluted aqueous HF solution for 10 min. Then, the cleaned silicon wafer was cut into two pieces. One was etched in a 5.0 mol/L HF solution containing 0.02 mol/L silver nitrate at 50 °C for 10 min in a conventional teflon-lined stainless steel vessel. The other was etched for 30 min with the same procedure. After the etching process, the two silicon wafers were rinsed with de-ionized water and blown dry in air. The thick silver film covering the silicon wafer with 30-min etching was detached for microstructural observation. A powder X-ray diffraction (XRD) spectrometer was used to characterize the silver dendrite. Data were collected on a Japan Rigaku D/Max-RA X-ray diffractometer with Cu K_α radiation ($\lambda = 1.54178$ Å). The morphology of the samples was characterized with a FEG JSM 6335 field-emission scanning electron microscope (SEM). All the measurements were performed at room temperature.

Figure 1 shows the SEM image of surface morphology of the silicon wafer etched for 10 min. It is found that the silver nanoclusters with diameters in the range of 100–300 nm are embedded in the Si nanowire array and tiny silver nanocrystals are attached to the apexes and walls of the Si nanowires. Formation of the silver nanoclusters and silver-capped Si nanowires can be understood on the basis of a self-assembled

✉ Fax: +86-25-8359-5535, E-mail: hkxlwu@nju.edu.cn
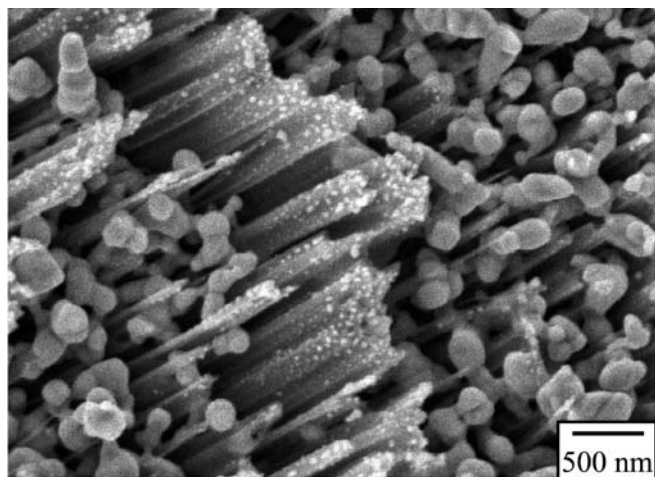
FIGURE 1   SEM image of surface morphology of the silicon wafer etched for 10 min, showing silver nanoclusters embedded in Si nanowire arrays and tiny silver nanocrystals attached to the apexes and walls of Si nanowires

localized microscopic electrochemical cell model [18]. At the initial stage, silicon etching and silver deposition occur simultaneously at the Si-wafer surface. The deposited silver atoms first form nuclei and then form nanoclusters, which are uniformly distributed on the surface of the silicon wafer. These silver nanoclusters and the Si areas surrounding these silver nuclei could respectively act as local cathodes and anodes in the electrochemical redox reaction process, which can be formulated as two half-cell reactions (1) and (2):

$$Ag^+ + e^- \rightarrow Ag \quad \text{and} \tag{1}$$

$$Si + 6F^- \rightarrow SiF_6^{2-} + 4e^- . \tag{2}$$

That is to say, numerous nanometer-sized free-standing electrolytic cells could be spontaneously assembled on the surface of the silicon wafer in aqueous HF solution. With the progress of silver deposition, the surrounding silicon acting as the anodes is etched away, while silver nanoclusters acting as the cathodes are successfully preserved and many of them are

dispersed in Si nanowire arrays. Thus, the presence of these nanoscale electrolytic cells leads to selective etching of the silicon substrate.

In the case of silver deposition, the etched silicon wafer was always covered with a layer of thick silver film, which is rather loose and could be easily detached from the surface of the silicon wafer. Figure 2 shows the SEM image of surface morphology of the silicon wafer etched for 30 min, from which the thick silver film has been detached. No noticeable silver nanoclusters are found in the Si nanowire arrays. Most of them diffuse onto the nearby pre-formed silver seeds above the etched Si nanowires along the pore channels in the nanowire network that is prepared in situ. Tiny silver nanocrystals attached to the apexes of the Si nanowires still exist. Tree-like structured Ag nanocrystals are found on the top of the Si nanowires, which can be more clearly observed from the detached thick silver film.

Figure 3a shows the SEM image of the tree-like silver dendrite from the thick silver film grown at 50 °C for 30 min. The diameters of stems for silver dendritic nanostructures are ~ 100 nm, which are the same as the sizes of the silver

a

b

FIGURE 2   SEM image of surface morphology of the silicon wafer etched for 30 min, showing no noticeable silver nanoclusters in the Si nanowire array but some chain-like Si nanostructures above the Si nanowire network
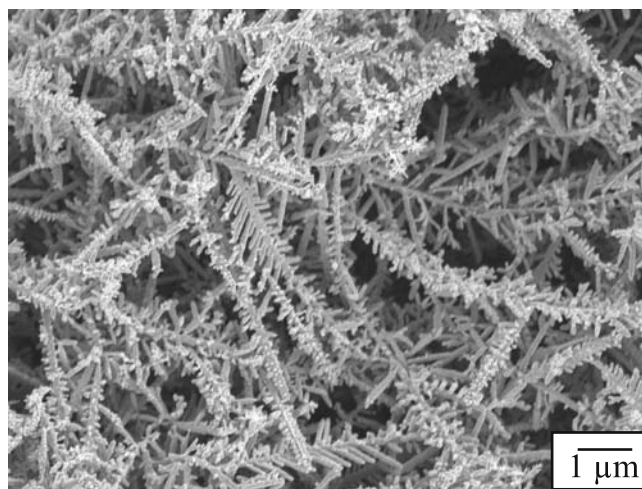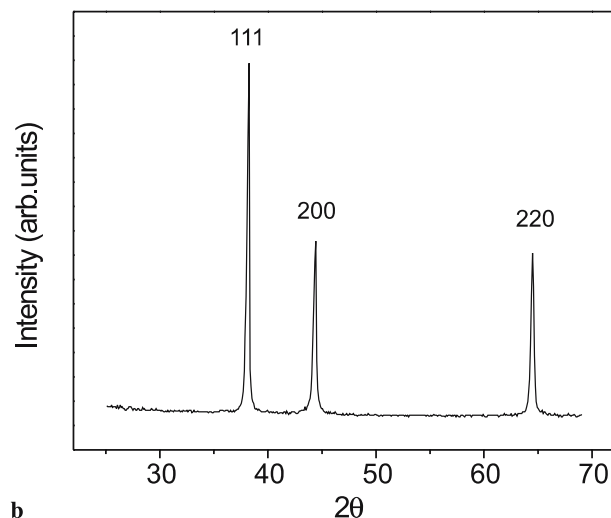
FIGURE 3   **a** SEM image of the tree-like silver dendrite grown at 50 °C for 30 min. **b** XRD pattern of the as-prepared nanostructured silver dendrite
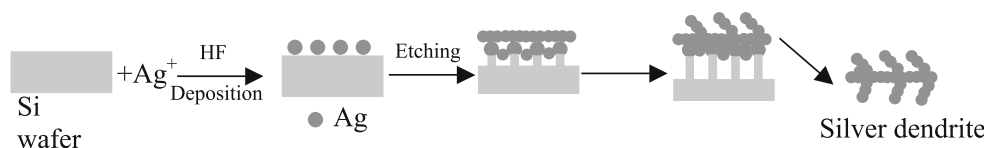
nanoclusters formed at the initial stage. Shapely stems, symmetrical branches, and leaves can be clearly observed.

Typical powder XRD patterns of the silver dendritic nanostructures are shown in Fig. 3b. The three diffraction peaks can be respectively indexed to the (111), (200), and (220) planes of face-centered-cubic (fcc) silver, with a lattice constant of $a = 4.080$ Å, which is in agreement with the reported value $a = 4.086$ Å (JCPDS 04-0783).

The tree-like silver nanostructures have been observed before [7–9]. However, the currently observed results are different from previous ones in many aspects. First, the ramification of the silver deposition has been greatly suppressed, and smooth leaves are generated on the substrate. Second, a periodic nanostructure is formed, which marks the evolution of the deposition and is beneficial to understanding the mechanism of electroless metal (silver) deposition.

The formation mechanism of these silver dendritic nanostructures observed can be schematically described in Fig. 4. At the beginning, the silicon etching and silver deposition occur simultaneously at the silicon surface. Many small flat honeycombs form around one tiny deposited silver nanocluster, that is to say, numerous nanosized honeycomb-like anodes and one silver nanocluster acting as a local cathode form an electrochemical cell [19]. At the same time, some formed silver nanoclusters also drop into the holes of the honeycombs. These cells could be self-assembled on the surface of the silicon wafer. The synchronous growth of silver dendrites should be considered within the framework of a DLA model [5], which involves in cluster formation by the adhesion of a particle with a random path to a selected seed on contact and allows the particle to diffuse and stick to the growing structure. In situ prepared honeycombs around the silver nanoclusters could be regarded as the template that is something like Xiao et al.'s work on ultrasonically assisted template synthesis of palladium and silver dendritic nanostructures [8]. During the initial stage, high concentrations of the silver salt and the reduction agent lead to reduction–nucleation–growth of silver nanoclusters at a lot of positions to form a chainlike network. With prolonging of the reaction duration, the concentrations of the silver salt and the reduction agent greatly decrease, the growth is mainly driven by decreasing surface energy, and thus the dendritic silver nanostructures are formed.

In fact, during the metal-deposition process in HF solution, metal nanoclusters generally have a tendency to coalesce and form a continuous grain film [18]. But, silver nanoclusters eventually form tree-like dendrites by consuming large quantities of superfluous deposited silver atoms, which must be accompanied by the appearance of silver vacancy defects. These silver vacancy defect centers have been considered to be the source of the 330-nm photoluminescence peak [20]. This kind of UV-emitting silver dendritic nanostructures can be expected to have favorable applications in optoelectronics [21].

In summary, unique silver dendritic nanostructures, with stems, branches, and leaves, have been self-organized via a simple electroless metal deposition method. Formation of the silver nanoclusters and silver-capped Si nanowires can be understood on the basis of a self-assembled localized microscopic electrochemical cell model. Using in situ prepared honeycombs around the silver nanoclusters as the template, the synchronous growth of silver dendrites is considered within the framework of the DLA model. The UV-emitting and symmetric structures of silver dendrites are promising for applications in optoelectronics and building blocks for assembling mini-functional devices of the next generation.

REFERENCES

1 L.M. Sander: Nature **322**, 789 (1986)
2 J. Nittmann, H.E. Stanley: Nature **321**, 663 (1986)
3 E. Ben-Jacob, P. Garik: Nature **343**, 523 (1990)
4 S.Z. Wang, H.W. Xin: J. Phys. Chem. B **104**, 5681 (2000)
5 T.A. Witten Jr., L.M. Sander: Phys. Rev. Lett. **47**, 1400 (1981)
6 P. Meakin: Phys. Rev. Lett. **51**, 1119 (1983)
7 Y. Zhou, S.H. Yu, C.Y. Wang, X.G. Li, Y.R. Zhu, Z.Y. Chen: Adv. Mater. **11**, 850 (1999)
8 J.P. Xiao, Y. Xie, R. Tang, M. Chen, X.B. Tian: Adv. Mater. **13**, 1887 (2001)
9 C. Bréchignac, P. Cahuzac, F. Carlier, C. Colliex, J. Leroux, A. Masson, B. Yoon, U. Landman: Phys. Rev. Lett. **88**, 196 103 (2002)
10 I.R. Gould, J.R. Lenhard, A.A. Muenter, S.A. Godleski, S.J. Farid: J. Am. Chem. Soc. **122**, 11 934 (2000)
11 Y.G. Sun, Y.N. Xia: Adv. Mater. **14**, 833 (2002)
12 H. Brune, C. Romalnexyk, H. Röder, K. Kern: Nature **369**, 469 (1994)
13 H. Brune, H. Röder, K. Bromann, K. Kern, J. Jacobsen, P. Stoltze, K. Jacobsen, J. Nørskov: Surf. Sci. **349**, L115 (1996)
14 P. Gorostiza, M.A. Kulandainathan, R. Diaz, F. Sanz, P. Allongue, J.R. Morante: J. Electrochem. Soc. **147**, 1026 (2000)
15 R. Sard, Y. Okinaka, H.A. Waggener: J. Electrochem. Soc. **136**, 462 (1989)
16 D.B. Wolfe, J.C. Love, K.E. Paul, M.L. Chabinyc, G.M. Whitesides: Appl. Phys. Lett. **80**, 2222 (2002)
17 A. Hilmi, J.H.T. Luong: Anal. Chem. **72**, 4677 (2000)
18 K.Q. Peng, Y.J. Yan, S.P. Gao, J. Zhu: Adv. Funct. Mater. **13**, 127 (2003)
19 T. Qiu, X.L. Wu, Y.F. Mei, G.J. Wan, P.K. Chu: (unpublished)
20 T. Qiu, X.L. Wu, X. Yang, G.S. Huang, Z.Y. Zhang: Appl. Phys. Lett. **84**, 3867 (2004)
21 H. Kind, H.Q. Yan, B. Messer, M. Law, P.D. Yang: Adv. Mater. **14**, 158 (2002)